Applied Physics B (2021) 127:2
https://doi.org/10.1007/s00340-020-07546-w

Applied Physics B
Lasers and Optics

Continuous-wave efficient cyan-blue Pr:$YAlO_3$ laser pumped by InGaN laser diode

Martin Fibrich[1,2] · Jan Šulc[1] · Richard Švejkar[1] · Helena Jelínková[1]

Received: 16 July 2020 / Accepted: 20 October 2020

Abstract
We report on the first continuous-wave quasi three-level laser emitting in the cyan-blue spectral range in praseodymium-doped oxide materials, as we believe. Pr:$YAlO_3$ crystal, cooled to the cryogenic temperatures, was used as an active medium. To minimize resonator losses, the cavity mirrors were directly deposited on the crystal faces to form a microchip geometry. More than half-Watt of the output power at 493 nm wavelength with a slope efficiency of 26% has been obtained under 3 W InGaN laser diode pumping at 447 nm wavelength.

1 Introduction

Trivalent praseodymium Pr^{3+} is the most established rare earth ion for direct generation of the laser radiation in the visible spectral range. Its energy level structure enables several transitions in the red, orange, green, and blue spectral region. Recent progress in the development of pump sources based on InGaN laser diodes (LD), usually used as an affordable alternative to optically pumped semiconductor lasers, allows to build compact and efficient Pr^{3+} solid-state lasers which can find applications, e.g., in the field of data storage, display technology, medicine, fluorescence microscopy, or spectroscopy.

Over the past decades, efficient Pr^{3+} laser operation at wavelengths spanning the whole visible spectrum has been demonstrated in fluoride crystals, such as $LiYF_4$ [1], $LiLuF_4$ [2], $LiGdF_4$ [3], KY_3F_{10} [4], BaY_2F_8 [5], LaF_3 [6], CaF_2 [7], and SrF_2 [8], as well as oxide materials such as $YAlO_3$ [9], $SrAl_{12}O_{19}$ [10], and $CaAl_{12}O_{19}$ [11]. Summary of the Pr^{3+} visible laser achievements is well presented in [12]. Most of these lasers were working in a four-level laser scheme (green, orange, and red laser transitions). However, the four-level laser scheme has inherently lower Stokes efficiency, so the maximum achievable overall efficiency is lower than that of lasers operating in three- or quasi-three-level scheme. From this perspective, the quasi-three-level Pr^{3+} laser research seems to be interesting [13]. So far, the efficient continuous-wave (CW) quasi three-level laser operation at cyan-blue laser transition has been demonstrated only in the Pr^{3+}:BaY_2F_8 and Pr^{3+}:$LiYF_4$ laser materials [13].

In our experiment, we paid attention to one of the most prominent Pr-doped oxide representatives, Pr:$YAlO_3$ (Pr:YAP) material, which proved to be worth alternative to Pr-fluorides. Compared to fluorides, this perovskite-type oxide crystal yield benefits from the excellent hardness (8.5–9 on the Mohs scale) and satisfactory thermal conductivity (not worse than 11 W m^{-1} K^{-1} at 300 K) [14]. In addition, YAP exhibits a positive value of the temperature coefficient dn/dT that can allow for a microchip laser geometry to be used [15, 16]. This particular geometry can be attractive for various applications in industry and medicine because of its compact and rugged design, combined with the potential for high efficiency and good beam quality.

The first observation of quasi-three-level cyan-blue Pr:YAP laser emission dates back to 1994 [17], where pulsed dye laser (pumped by a tripled Nd:YAG or excimer laser) was used as an excitation source. The system was operated at cryogenic temperatures because the Pr:YAP cyan-blue laser transition around 491 nm terminates on the second 52 cm^{-1} Stark component of the ground state manifold [17] which starts to be substantially thermally populated at higher temperatures. However, the overall efficiency of the laser system was very low and there are no reports about the efficient

✉ Martin Fibrich
martin.fibrich@fjfi.cvut.cz

[1] Faculty of Nuclear Sciences and Physical Engineering, Czech Technical University in Prague, Brehova 7, 115 19 Prague, Czech Republic

[2] Institute of Physics ASCR, ELI-Beamlines, Na Slovance 1999/2, 182 21 Prague, Czech Republic

Published online: 25 November 2020

and/or CW cyan-blue Pr^{3+} laser operation utilizing oxide laser hosts.

So, in this letter, we report the first results on the efficient CW cyan-blue laser emission of Pr^{3+}-doped oxide material, Pr:YAP crystal, at 493 nm wavelength ($^3P_0 \rightarrow {}^3H_4$ laser transition; see Fig. 1), as well as the Pr:YAP spectroscopy at 4 K crystal temperature. To operate such a laser, cooling of the crystal at cryogenic temperatures (4 – 40 K) had to be applied to overcome the reabsorption losses originating from the thermally coupled higher Stark levels of the $^3H_4$ ground-state manifold, and to reach a gain under InGaN LD pumping with the maximum available pump power of 3 W at 447 nm wavelength. As a result, 514 mW of the output power at 493 nm was extracted from the crystal. The corresponding slope efficiency with respect to absorbed pump power was 26%.

2 Spectroscopic characteristics

Polarization resolved ground-state absorption spectra of the 5 mm long 0.6 at.% doped b-cut (according to Pbnm notation) Pr:YAP sample at cryogenic temperatures down to 4 K were measured by Shimadzu spectrophotometer UV-3600 (slide width 0.5 nm, sampling 0.05 nm). Processed spectra in terms of absorption coefficients are shown in Fig. 2. It should be remarked that at 4 K crystal temperature, the 447 nm laser transition ($^3H_4 \rightarrow {}^3P_2$), easily available by the LDs, represents one of the most efficient way how to pump Pr:YAP crystal. In addition, absorption coefficient of that transition at 4 K is more than two times higher if compared

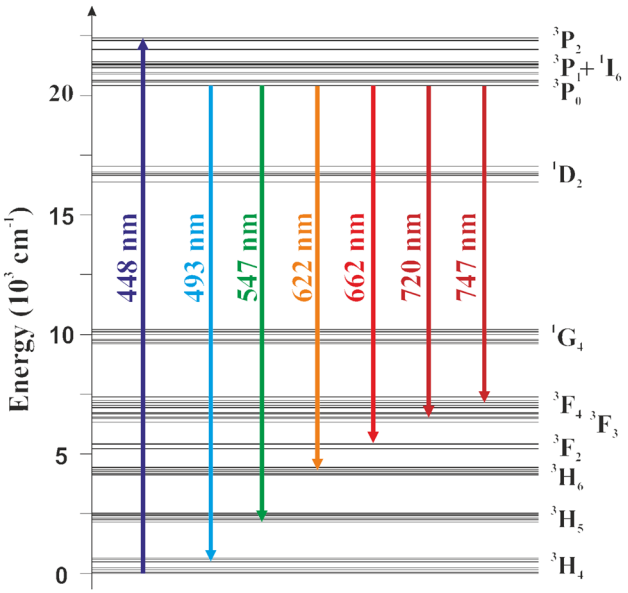

Fig. 1 Simplified 4f-energy level structure of Pr^{3+} ion

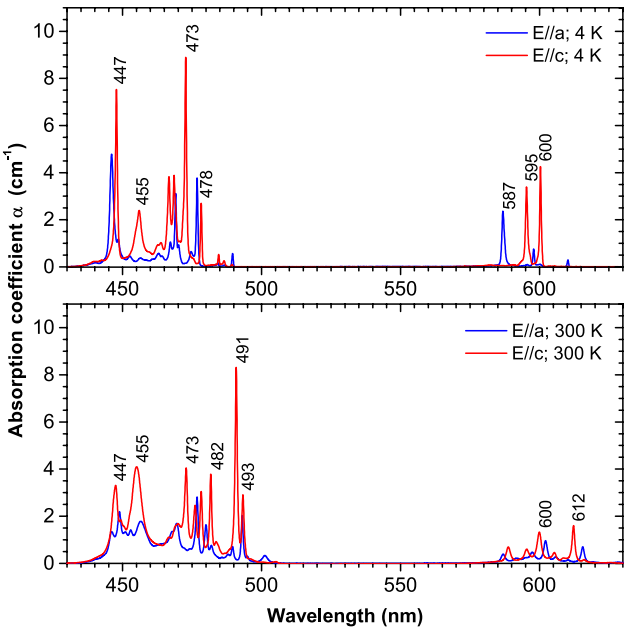

Fig. 2 Polarization-resolved Pr(0.6 at.%):YAP absorption spectra comparison at cryogenic and room temperature

with room temperature and the absorption line width is sufficient to accept LD emission even at 4 K temperature. Notice that the line with the highest absorption coefficient at room temperature (491 nm) disappears at 4 K.

Polarization-resolved emission spectra were measured by fiber coupled spectrometer (StellarNet BLACK-Comet C-50) operated within the 185–840 nm wavelength range, in the direction of the crystal longitudinal axis, together with oriented wire grid polarizer. To shield an unabsorbed InGaN LD excitation radiation, a cut-off filter was employed. Emission cross sections were calculated with the help of the Füchtbauer–Ladenburg formula; see Fig. 3.

The upper state-level lifetime of the Pr:YAP sample was evaluated from the decay time characteristic measurements after the crystal excitation by 50 µs LD pulse. To find the fluorescence decay time, the experimental data (fluorescence intensity recorded by Si-detector and oscilloscope) were fitted by a single-exponential curve. Only data recorded after the end of the excitation pulse were taken into account, so that the excitation signal did not affect the shape of the fluorescence decay curve. To be sure the recorded signal originates from the upper laser level $^3P_0$ only, the fluorescence signal was monitored behind the band-pass filter transparent in the range ~500–850 nm. The temporal response of the fluorescence recording system was better than 0.1 µs (detector capacity 2 pF, oscilloscope input capacity 13 pF, terminator resistance 5 kΩ), which can in principle affect the measured data, but not significantly and independently on temperature of the sample. From this reason we did not apply any deconvolution on the recorded data before fitting

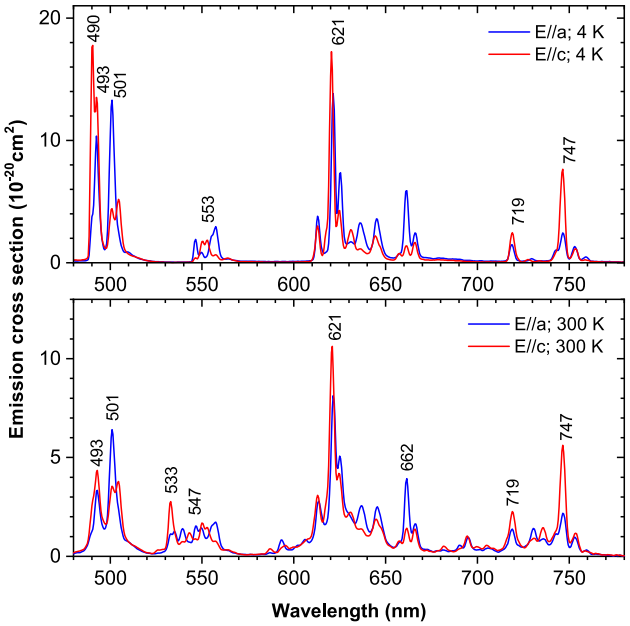

Fig. 3 Polarization-resolved Pr(0.6 at.%):YAP emission spectra comparison at cryogenic and room temperature

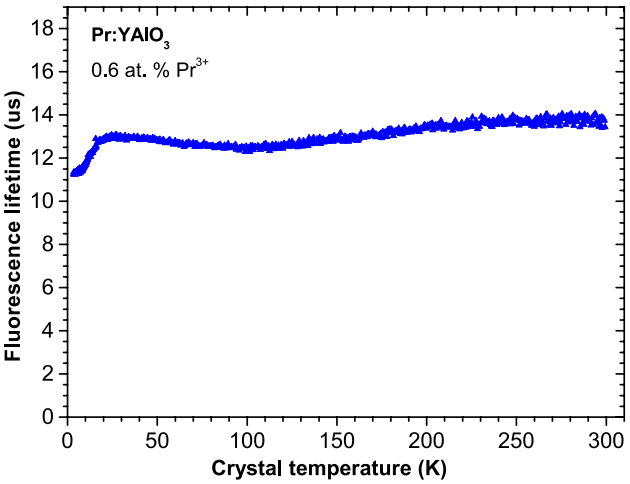

Fig. 4 Fluorescence lifetime as a function of Pr:YAP crystal temperature

to eliminate the influence of the detection system response time. The fluorescence lifetime determined for the crystal temperatures within 4–300 K range is shown in Fig. 4. It can be seen there are only small variation in the Pr:YAP lifetime with respect to the crystal temperature; the values oscillate between ~11.2 µs at 4 K to ~13.8 µs at room temperature (300 K). One would expect the excited-state lifetime should increase with the decrease of temperature because of less efficient non-radiative processes, such as the non-radiative decay rate based on the energy gap to the adjacent lower energy level. Nevertheless, the influence of temperature on the fluorescence lifetime is not so straightforward for lanthanide ions and could be strongly material dependent (lifetime drop with decreasing temperature was observed, e.g., for Tm:CaF_2 [18], or for Nd:YAG [19]). The decrease in Pr:YAP lifetime below 20 K can be explained by the cross relaxation increasing because at that very low temperatures there are almost no phonon-assisted cross-relaxation processes. So, as the temperature decreases, the strength of the transition cross sections are increasing and if there is a near ideal overlap between the lower Stark levels in the respective initial manifold ($^3P_0$, $^3H_4$) and any of the terminal levels, then, in fact, the strength of the cross relaxation rate (based upon the convolution of the spectral overlap for transitions between $^3P_0 \rightarrow {}^1G_4$ and $^3H_4 \rightarrow {}^1G_4$ or $^3P_0 \rightarrow {}^1D_2$ and $^3H_4 \rightarrow {}^3H_6$) can be increasing. However, it would require further investigations to confirm this, for example, to measure the lifetime of a lower concentration crystal, where the ion spacing is greater, reducing the coupling strength.

3 Experimental arrangement and results

To realize cyan-blue Pr:YAP laser, 0.6 at.% doped Pr:YAP active medium grown by the Czochralski method was used. The sample was high quality, free of crack or twins, ϕ 5 mm×5 mm in dimension, and it was cut along the b-axis (according to Pbnm notation). Both facets polished in laser quality were perpendicular to the laser radiation propagation direction. To minimize resonator losses resulting in a lower threshold and a higher system efficiency, microchip geometry realized by cavity mirrors directly deposited as a dielectric films on the crystal faces has been employed. The microchip pump side (pump mirror) was highly transmitted for the incident pump radiation ($T > 90\%$ at room temperature), and highly reflective ($R > 99.8\%$ at room temperature) for the generated radiation. The reflectivity of the opposite side (output coupler) was $R \sim 98\%$ (at room temperature) for the wavelength range of interest around 490 nm. Moreover, the opposite facet was partially reflective ($R \sim 35\%$ at room temperature) for the pump radiation to increase the overall absorption efficiency of the crystal.

To allow the laser operation at cryogenic temperatures, the active medium was placed in the He-cryostat (Optistat-Dry BLV cryostat; Oxford Instruments) with uncoated CaF_2 windows. The crystal temperature could be controlled at any value within the 4–300 K range. The laser crystal wrapped into a high-purity indium foil (100 µm thick) was clamped in a holder made from high-purity copper. The indium foil was used to improve a thermal contact between the crystal and the cupreous holder. The holder was then directly mounted to a cryostat cold finger. Thanks to a birefringent character

of the YAP laser host, the thermally induced birefringence does not degrade the laser performance.

A pump process was realized by an InGaN LD (NICHIA Corporation) providing a linearly polarized beam centred at ~447 nm. The maximum output power available at this wavelength was 3 W and the pump beam quality was determined to be $M_x^2 \sim 2.7$ and $M_y^2 \sim 8.1$ (x/y denotes the fast/slow axis) with the 1.7 nm linewidth (FWHM).

The laser experiment setup is schematically illustrated in Fig. 5. The InGaN LD output radiation was collimated by an aspherical lens ($f = 4.5$ mm, 0.55 NA, ARC = 400–600 nm) and after going through the achromatic half-wave plate for the 400–800 nm wavelengths (Thorlabs Inc.), the radiation was focused into the active medium by a lens with the 60 mm focal length, resulting in a spot size of about 60 µm in radius. The half-wave plate fixed in a rotation mount was used to align the polarization of the excitation beam parallel to the laser crystal axis providing the highest absorption cross section, and thus to reach a high absorption efficiency in the active medium. Laser output radiation was detected behind the cut-off filter.

Pr:YAP input–output laser characteristic in the cyan-blue spectral range at 493 nm is depicted in Fig. 6. A maximal output power of 514 mW was reached when the crystal was cooled down to 4 K. The corresponding oscillation threshold and slope efficiency related to the absorbed pump power were 500 mW and 26%, respectively. Maximal pump power absorbed in the crystal in a single pass was estimated to be 84% at 4 K crystal temperature. The polarization of the 493 nm laser radiation corresponded to $E \parallel c$ polarization. Degree of this linear polarization (regarding a definition in e.g. [20]) was determined to be > 99.5% (extinction ratio of the polarizer used was > 800:1 over the wavelength range 420–700 nm). It should be noted that the absorbed pump power in the crystal is the upper estimation. We suppose that the back propagating pump radiation reflected from the microchip output side is fully absorbed and fully contributed to the laser generation. So, as a consequence, the slope efficiency is the lower estimation and, in fact, the value of

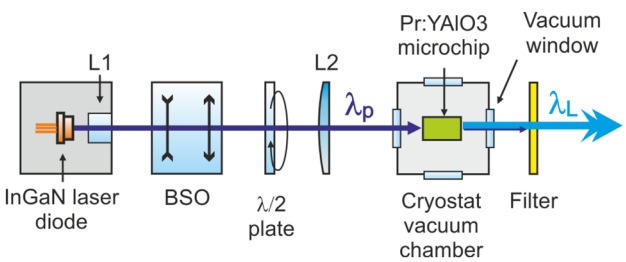

Fig. 5 Schematic layout of longitudinally InGaN LD pumped Pr:YAP microchip laser system operated at cryo-temperatures at 493 nm; λ_p—pump wavelength, λ_L—generated wavelength, L1—collimating lens, L2—focusing lens

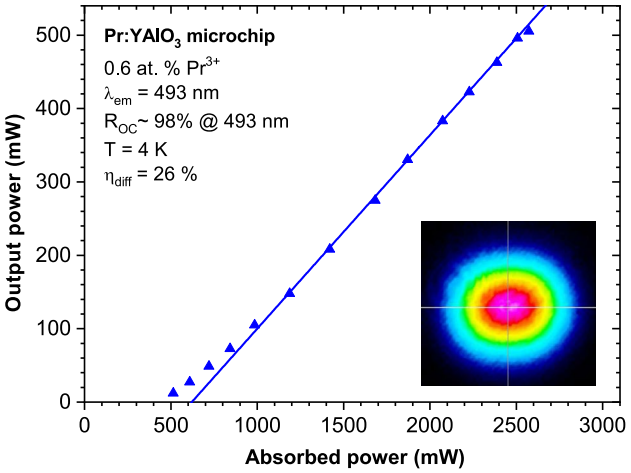

Fig. 6 Output characteristic of cyan-blue Pr:YAP microchip laser at 4 K crystal temperature; inset—spatial beam profile at maximal output power

the slope is probably higher. The laser operated close to the single transversal TEM_{00} mode (see inset in Fig. 6).

Furthermore, the maximal laser output power as a function of crystal temperature was evaluated, as shown in Fig. 7. The laser emission at 493 nm was observed up to ~23 K crystal temperature; after that the Pr:YAP laser started to operate at 553 nm in the green region. It can be explained as follows; when the crystal temperature is going up, the thermal population of the terminal Pr:YAP laser level (higher Stark level of the $^3H_4$ ground state manifold) is exponentially increasing

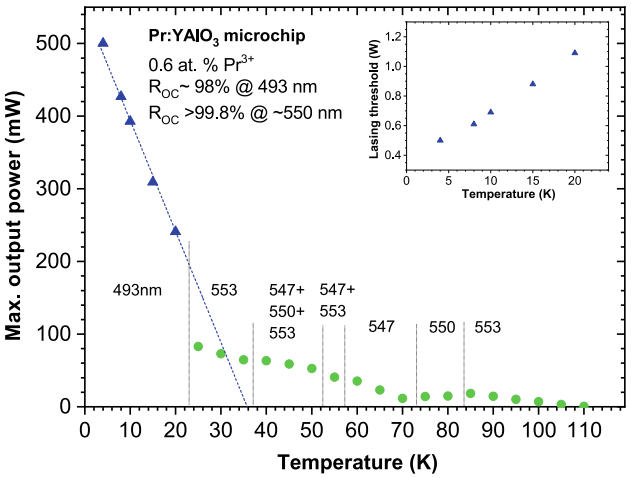

Fig. 7 Maximal Pr:YAP cyan-blue microchip laser output power as a function of crystal temperature; vertical dotted lines delimited temperature regions with the respective emission wavelengths given by the numbers. Several numbers in the given region mean that the Pr:YAP microchip laser generated at several wavelengths simultaneously. Inset: lasing threshold for 493 nm emission with respect to crystal temperature

and the laser tends to switch its operation from the quasi-three level regime (cyan-blue laser operation) to energetically more favorable four-level regime, if it is possible. In our case, the reflectivity of both crystal facet coatings for wavelengths around 550 nm was $R > 99.8\%$ at room temperature, so the green laser generation was enabled. Nevertheless, by proper design of the resonator mirrors allowing for the low reflectivity at the green wavelengths (as well as at another possible Pr^{3+} emission lines in the visible spectral region), resulting in a high cavity losses and suppression of the laser emission at the non-preferred laser transitions, one can expect the cyan-blue laser operation up to ~35 K crystal temperature—see the extrapolated linear fit of the cyan-blue data in Fig. 7. This corresponds very well with the fact that the crystal temperature is driving mainly the lasing threshold (see inset in Fig. 7). It should be remarked that although the Pr:YAP absorption in the temperature range 4–300 K varies significantly, the variation of LD radiation absorption at 447 nm ($E \parallel c$) important for presented laser experiment is not so strong, especially for temperatures below 30 K (see Fig. 8). Therefore, the results in Fig. 7 are presented as measured without any correction to LD pump absorption variation with temperature.

For the sake of completeness, it should be mentioned here that almost 100 mW of the green output power was obtained at 25 K at 553 nm wavelength. The output power presented in Fig. 7 was taken as a doubled output power measured behind the output coupler because the reflectivities of the pump and out-coupling mirrors were comparable in the green region around 550 nm (the reflectivity curves of the mirrors coated on the crystal facets were almost flat in the green spectral range with the reflectivity greater than 99.8%). The corresponding slope efficiency was 8%. Keep in mind the green laser output power refers, in fact, to the closed resonator where only small part of the intracavity green power is coupled out. By optimizing the output coupler reflectivity for this spectral region, we expect the output power close to half-Watt in the green. The observed competition between the green wavelengths (Fig. 7) can be explained by a different rate of variation in cross emission peak values with respect to temperature.

Based on the presented Pr:YAP emission spectra at 4 K (see Fig. 3), one would expect blue laser generation at the wavelength with the highest emission cross section, i.e., 490 nm. The reason why the Pr:YAP prefers to lase at 493 nm transition is given mainly by the reabsorption losses. As shown in Fig. 9, describing the dependence of the absorption coefficient maxima at crystal temperature, there is not-negligible absorption at 490 nm transition even at 4 K crystal temperature, while for 493 nm the reabsorption becomes significant from ca. 40 K. So, gain-to-loss ratio in the temperature range 4–30 K is practically infinity (if we neglect the scattering losses inside the microchip laser) for the lasing 493 nm wavelength, because the Pr^{3+} re-absorption at the lasing wavelength is close to zero (see Fig. 9) and the laser is de facto operating in four-level scheme.

4 Discussion and conclusion

To conclude, the first CW quasi three-level laser based on Pr^{3+}-ion doped oxide material is presented, to the best of our knowledge. Using Pr:YAP microchip crystal (resonator mirrors directly coated on the crystal facets), the cyan-blue laser emission at 493 nm wavelength ($^3P_0 \rightarrow {}^3H_4$ laser transition) was reached under InGaN LD pumping. Cooling of the crystal to cryogenic temperatures was required to minimize the reabsorption losses originating from the thermally populated terminal laser level (higher Stark level of the ground state manifold $^3H_4$). A maximal output power of 514 mW was

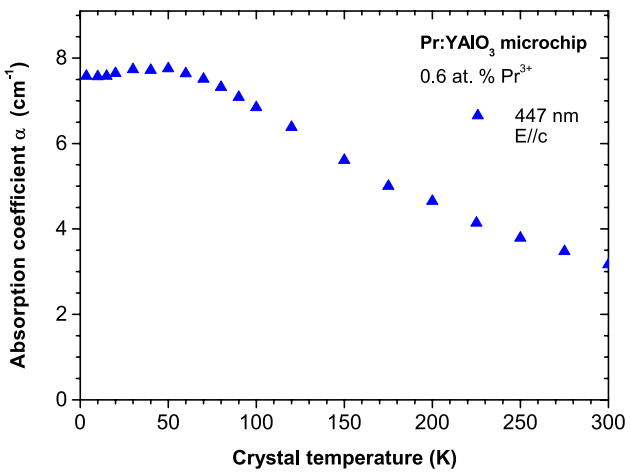

Fig. 8 Peak absorption coefficient amplitude at 447 nm as a function of crystal temperature for $E \parallel c$ polarization

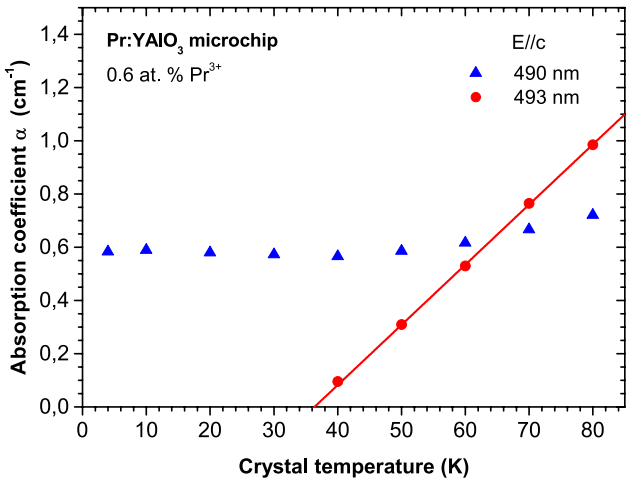

Fig. 9 Peak absorption coefficient amplitude of the selected laser transitions as a function of crystal temperature

obtained with a slope efficiency of 26% (with respect to absorbed pump power) at crystal temperature of 4 K.

In addition, Pr:YAP laser generation in the green spectral range at 553 nm wavelength was demonstrated. As we know, this is the first report about the laser emission at 553 nm wavelength from the perovskite-type oxide material. Nevertheless, further investigation will be needed to examine carefully the Pr:YAP laser performances in the green spectral range at cryogenic temperatures starting at 4 K, which is one of our next experimental goals.

It should be also noted that the investigations performed in this work were not fully optimized for efficiency. Lower slope efficiency with respect to Stokes efficiency can be explained by non-optimal overlapping of the cavity and pump mode rather than by the significant losses in the microchip. The overlapping was estimate to be about 35%, which was affected, among other things, by the strong ellipticity of the pump beam. Employing beam shaping optics should help to improve that. In addition, fine positioning/tilting of the crystal in the cryostat with respect to pump beam would be also worthwhile. Moreover, further improvement of the laser output characteristics can be expected by optimizing the output coupler reflectivity as well as the pump beam quality, e.g. by utilizing an optically pumped frequency doubled semiconductor laser exhibiting excellent beam quality ($M^2_{x,y} \approx 1$) allowing to reach a higher inversion densities with the same available pump power.

In connection with the good thermo-mechanical properties and possibility of laser operation spanning the whole visible spectral range (near-infrared, deep red, red, orange, and green wavelengths have already been demonstrated [16, 20, 21]), the Pr:YAP crystal presents an interesting alternative to the Pr^{3+} doped fluoride hosts. The fact that cryogenic temperatures are required to realize efficient Pr:YAP laser emission at some allowed laser transitions (green and cyan-blue) should not represent any significant limitation in the present day from the practical point of view. Nowadays, He-based cryostat are very compact, stable, and easy-to-handle devices, with the non-stop operation capability. This together with easy implementation of the microchip geometry (due to the positive value of the temperature coefficient *dn*/*dT*) opens up the possibilities for various applications in medicine or industry.

Funding Centre of Advanced Applied Natural Sciences (CZ.02.1.01/0.0/0.0/16_019/0000778).

References

1. P.W. Metz, F. Reichert, F. Moglia et al., High-power red, orange, and green Pr^{3+}:$LiYF_4$ lasers. Opt. Lett. **39**, 3193–3196 (2014)
2. A. Richter, E. Heumann, G. Huber et al., Power scaling of semiconductor laser pumped Praseodymium-lasers. Opt. Express **15**, 5172–5178 (2007)
3. F. Cornacchia, A.D. Lieto, M. Tonelli et al., Efficient visible laser emission of GaN laser diode pumped Pr-doped fluorideschеelite crystals. Opt. Express **16**, 15932–15941 (2008)
4. P. Camy, J.L. Doualan, R. Moncorgé et al., Diode-pumped Pr^{3+}:KY_3F_{10} red laser. Opt. Lett. **32**, 1462–1464 (2007)
5. A. Sottile, D. Parisi, M. Tonelli, Multiple polarization orange and red laser emissions with Pr:BaY_2F_8. Opt. Express **22**, 13784–13791 (2014)
6. F. Reichert, F. Moglia, D.-T. Marzahl et al., Diode pumped laser operation and spectroscopy of Pr^{3+}:LaF_3. Opt. Express **20**, 20387–20395 (2012)
7. H. Yu, D. Jiang, F. Tang et al., Enhanced photoluminescence and initial red laser operation in Pr:Ca F_2 crystal via co-doping Gd^{3+} ions. Mater. Lett. **206**, 140–142 (2017)
8. T.T. Basiev, V. Konyushkin, D.V. Konyushkin et al., First ceramic laser in the visible spectral range. Opt. Mater. Express **1**, 1511–1514 (2011)
9. M. Fibrich, H. Jelínková, J. Šulc et al., Diode-pumped Pr:YAP lasers. Laser Phys. Lett. **8**, 559–568 (2011)
10. M. Fechner, F. Reichert, N.-O. Hansen et al., Crystal growth, spectroscopy, and diode pumped laser performance of Pr, Mg:$SrAl_{12}O_{19}$. Appl. Phys. B **102**, 731–735 (2011)
11. F. Reichert, D.-T. Marzahl, G. Huber, Spectroscopic characterization and laser performance of Pr, Mg:$CaAl_{12}O_{19}$. J. Opt. Soc. Am. B **31**, 349–354 (2014)
12. C. Kränkel, D.-T. Marzahl, F. Moglia et al., Out of the blue: semiconductor laser pumped visible rare-earth doped lasers. Laser Photonics Rev. **10**(4), 548–568 (2016)
13. P.W. Metz, K. Hasse, D. Parisi et al., Continuous-wave Pr^{3+}:BaY_2F_8 and Pr^{3+}:$LiYF_4$ lasers in the cyan-blue spectral region. Opt. Lett. **39**, 5158–5161 (2014)
14. A.A. Kaminskii, *Crystalline Lasers: Physical Processes and Operating Schemes* (CRC Press, Boca Raton, 1991), p. 571
15. M. Fibrich, H. Jelínková, J. Šulc et al., Pr:$YAlO_3$ microchip laser. Opt. Lett. **35**, 2556–2557 (2010)
16. M. Fibrich, J. Šulc, H. Jelínková, Pr:$YAlO_3$ laser generation in the green spectral range. Opt. Lett. **38**, 5024–5027 (2013)
17. M. Malinowski, M.F. Joubert, R. Mahiou et al., Visible laser emission of Pr^{3+} in various hosts. J. Phys. IV Fr. **04**(C4), C4-541–C4-544 (1994)
18. J. Reiter, J. Körner, J. Pejchal et al., Temperature dependent absorption and emission spectra of Tm:CaF_2. Opt. Mater. Express **10**, 2142–2158 (2020)
19. J. Sulc, M. Nemec, H. Jelinkova et al., Temperature influence on microchip lasers based on Nd:YAG crystal, in *Solid State Lasers XXVIII: Technology and Devices*, vol. 10896, ed. by W.A. Clarkson, R.K. Shori (International Society for Optics and Photonics, SPIE, Washington, 2019), pp. 303–312
20. B. García-Cámara, F. González, F. Moreno, Linear polarization degree for detecting magnetic properties of small particles. Opt. Lett. **35**, 4084–4086 (2010)
21. H. Chen, H. Uehara, H. Kawase et al., Efficient Pr:$YAlO_3$ lasers at 622 nm, 662 nm, and 747 nm pumped by semiconductor laser at 488 nm. Opt. Express **28**, 3017–3024 (2020)
22. M. Fibrich, H. Jelínková, Power-scaled Pr:$YAlO_3$ laser at 747 and 720 nm wavelengths. Laser Phys. Lett. **10**, 035801 (2013)